ANL/RA/CP--84335

Contributed Paper to be submitted for ANS Portland topical meeting (M&C) in April 1995.

PERTURBATION THEORY BASED ON THE VARIATIONAL NODAL TRANSPORT METHOD IN X-Y-Z GEOMETRY*

Kirsten F. Laurin-Kovitz[a]
Northwestern University
Department of Mechanical Engineering
Evanston, IL 60208

E.E. Lewis
Northwestern University
Department of Mechanical Engineering
Evanston, IL 60208

*Work supported by the U.S. Department of Energy, Nuclear Energy Programs under Contract W-31-109-ENG-38.

[a]Laboratory Graduate Participant, Argonne National Laboratory, Reactor Analysis Division, Argonne, IL 60439.

PERTURBATION THEORY BASED ON THE VARIATIONAL NODAL TRANSPORT METHOD IN X-Y-Z GEOMETRY

Kirsten F. Laurin-Kovitz[a]
Northwestern University
Department of Mechanical Engineering
Evanston, IL 60208
(708)252-4840
kkovitz@anl.gov

E.E. Lewis
Northwestern University
Department of Mechanical Engineering
Evanston, IL 60208
(708)491-3579
e-lewis@nwu.edu

ABSTRACT

A perturbation method based on the Variational Nodal Method[1] (VNM) of solving the neutron transport equation is developed for three-dimensional Cartesian geometry. The method utilizes the solution of the corresponding adjoint transport equation to calculate changes in the critical eigenvalue due to changes in cross sections. Both first order and exact perturbation theory expressions are derived. The adjoint solution algorithm has been formulated and incorporated into the VNM option of the Argonne National Laboratory DIF3D production code.[2] The perturbation method is currently implemented as a post-processor to the VNM option of the DIF3D code. To demonstrate the efficacy of the method, example perturbations are applied to the Takeda Benchmark Model 1. In the first perturbation example, the thermal capture cross section is increased within the core region. For the second perturbation example, the increase in the thermal capture cross section is applied in the control rod region. The resulting changes in the critical eigenvalue are obtained by direct calculation in the VNM and compared to the change approximated by the first order and exact theory expressions from the perturbation method. Exact perturbation theory results are in excellent agreement with the actual eigenvalue differences calculated in the VNM. First order theory holds well for sufficiently small perturbations.

I. INTRODUCTION

Perturbation methods are frequently used in the design and analysis of nuclear reactors to calculate the effects of small changes in cross sections or other reactor characteristics on the critical state of the reactor. Fine mesh diffusion and discrete ordinates codes currently in use incorporate a corresponding perturbation method. As nodal methods become increasingly popular the need to develop corresponding perturbation methods becomes evident.

In order to develop such methods, the solution to the adjoint equation must first be formulated. With some nodal methods, the solution of the adjoint problem presents a difficulty; the physical adjoint, obtained by discretizing the adjoint equation is not the same as the mathematical adjoint, obtained by taking the transpose of the coefficient matrix which results from discretizing the forward equation. The existing nodal computational algorithms require the physical adjoint while the perturbation method requires the mathematical adjoint. Consequently, similarity transforms or related techniques must be applied to relate the physical and mathematical adjoints. To date, few nodal methods incorporate adjoint solutions and those methods which do, include them only for the diffusion approximation.[3,4,5,6,7]

In contrast, the physical and mathematical adjoints are identical for both diffusion and transport approximations in the Variational Nodal Method. In previous work, we have presented an adjoint solution algorithm for the VNM for both diffusion and transport approximations and demonstrated its use for two-dimensional perturbation problems.[8,9] Here, we derive both the adjoint algorithm and the perturbation method for calculating changes in the critical

---

[a]Laboratory Graduate Participant at Argonne National Laboratory, Reactor Analysis Division, Argonne, IL 60439.

eigenvalue for three-dimensional Cartesian geometry. Both exact theory and first order theory perturbation methods are developed and illustrated.

The remaining sections of this paper are organized as follows. Section II contains the derivation of the solution algorithm for the adjoint transport equation in three dimensions. In section III we derive the three-dimensional perturbation expressions for both exact and first order theory. Section IV contains perturbation examples based on the three-dimensional Takeda Benchmark Model 1. The final section includes a discussion of the results and explores future development of the perturbation method for the VNM.

II. FORWARD AND ADJOINT EQUATIONS

The continuous, within-group forward transport equation with isotropic scattering is:

$$[\hat{\Omega}\bullet\vec{\nabla} + \sigma(\vec{r})]\,\Psi(\vec{r},\hat{\Omega}) = S(\vec{r},\hat{\Omega}) + \sigma_S \int d\hat{\Omega}\,\Psi(\vec{r},\hat{\Omega}) \tag{1}$$

where $\vec{r}$ is a three-dimensional vector in space, σ and σ_s are the total and scattering cross sections and S is the group source. The continuous, within-group adjoint transport equation with isotropic scattering is:

$$[-\hat{\Omega}\bullet\vec{\nabla} + \sigma(\vec{r})]\,\Psi^*(\vec{r},\hat{\Omega}) = S^*(\vec{r},\hat{\Omega}) + \sigma_S \int d\hat{\Omega}\,\Psi^*(\vec{r},\hat{\Omega}) \tag{2}$$

where $\vec{r}$, σ, σ_s are the same as in the forward equation and S* is the adjoint group source.

We divide the flux into even- and odd-parity components, ψ and χ,

$$\begin{aligned}\psi(\vec{r},\hat{\Omega}) &= \tfrac{1}{2}\,[\,\Psi(\vec{r},\hat{\Omega}) + \Psi(\vec{r},-\hat{\Omega})]\ ,\\ \chi(\vec{r},\hat{\Omega}) &= \tfrac{1}{2}\,[\,\Psi(\vec{r},\hat{\Omega}) - \Psi(\vec{r},-\hat{\Omega})]\ .\end{aligned} \tag{3}$$

Likewise, the adjoint flux is divided into even- and odd-parity components, ψ^* and χ^*,

$$\begin{aligned}\psi^*(\vec{r},\hat{\Omega}) &= \tfrac{1}{2}\,[\,\Psi^*(\vec{r},\hat{\Omega}) + \Psi^*(\vec{r},-\hat{\Omega})]\ ,\\ \chi^*(\vec{r},\hat{\Omega}) &= \tfrac{1}{2}\,[\,\Psi^*(\vec{r},\hat{\Omega}) - \Psi^*(\vec{r},-\hat{\Omega})]\ .\end{aligned} \tag{4}$$

Substituting (3) and (4) into (1) and (2) respectively, we obtain the second order even-parity form of the forward and adjoint transport equations.

$$-\hat{\Omega}\bullet\vec{\nabla}\,\frac{1}{\sigma}\,\vec{\nabla}\psi(\vec{r},\hat{\Omega}) + \sigma\psi(\vec{r},\hat{\Omega}) = \sigma_S\,\phi(\vec{r}) + S(\vec{r}), \tag{5}$$

$$-\hat{\Omega}\bullet\vec{\nabla}\,\frac{1}{\sigma}\,\vec{\nabla}\psi^*(\vec{r},\hat{\Omega}) + \sigma\psi^*(\vec{r},\hat{\Omega}) = \sigma_S\,\phi^*(\vec{r}) + S^*(\vec{r})\ . \tag{6}$$

In the VNM, we construct a functional whose Euler-Lagrange equation is the second order even-parity transport equation

$$F[\psi,\chi] = \sum_n \left(\int_n dV \left\{ \int d\Omega \left[\frac{1}{\sigma}(\hat{\Omega}\bullet\vec{\nabla}\psi_n)^2 + \sigma\psi_n^2 \right] - \sigma_S\,\phi_n^2 - 2\,\phi_n\,s \right\} + 2\sum_m \int d\Gamma \int d\Omega\,\hat{n}\bullet\hat{\Omega}\,\psi_n\chi_m \right) \tag{7}$$

where n is the node index. Similarly, we can construct a functional whose Euler-Lagrange equation is the adjoint transport equation

$$F^*[\psi^*,\chi^*] = \sum_n \left[\int dV \left\{ \int d\Omega \left[\frac{1}{\sigma} (\hat{\Omega}\bullet\vec{\nabla}\psi_n^*)^2 + \sigma\psi_n^{*2} \right] - \sigma_S \phi_n^{*2} - 2\phi_n^* s^* \right\} - 2\sum_m \int d\Gamma \int d\Omega\, \hat{n}\bullet\hat{\Omega}\, \psi_n^* \chi_m^* \right] \quad (8)$$

Once we have the functionals for the forward and adjoint fluxes, we apply a classical Ritz procedure and construct approximations of the functionals. The even- and odd-parity forward and adjoint fluxes are approximated by the product of a vector of known trial functions in space and angle and a vector of unknown coefficients:

$$\psi_n(\vec{r},\hat{\Omega}) = \mathbf{f}(\vec{r},\hat{\Omega})\zeta_n ,$$
$$\chi_n(\vec{r},\hat{\Omega}) = \mathbf{h}(\vec{r},\hat{\Omega})\chi_n \quad (9)$$
$$\psi_n^*(\vec{r},\hat{\Omega}) = \mathbf{f}(\vec{r},\hat{\Omega})\zeta^*_n ,$$
$$\chi_n^*(\vec{r},\hat{\Omega}) = \mathbf{h}(\vec{r},\hat{\Omega})\chi^*_n \quad (10)$$

where, ζ and χ, ζ^* and χ^* are the even- and odd-parity forward and adjoint angular flux coefficient vectors. If the coefficients are expressed in terms of global vectors through the Boolean transforms,

$$\zeta_n = \Lambda_n \zeta , \qquad \chi_n = \Pi_n \chi ,$$

and

$$\zeta_n^* = \Lambda_n \zeta^* , \qquad \chi_n^* = \Pi_n \chi^* ,$$

the functionals reduce to the algebraic expressions

$$F[\zeta,\chi] = \zeta^T \mathbf{A}\zeta - 2\zeta^T \mathbf{s} + 2\zeta^T \mathbf{M}\chi \quad (11)$$

and

$$F^*[\zeta^*,\chi] = \zeta^{*T}\mathbf{A}\zeta^* - 2\zeta^{*T}\mathbf{s}^* - 2\zeta^{*T}\mathbf{M}\chi^* .$$

The global matrices **A** and **M** are superpositions of the nodal matrices containing space-angle integrals of the known trial functions.

$$\mathbf{A} = \sum_n \Lambda_n^T \mathbf{A}_n \Lambda_n ,$$
$$\mathbf{M} = \sum_n \Lambda_n^T \mathbf{M}_n \Pi_n , \quad (12)$$
$$\mathbf{s} = \sum_n \Lambda_n^T \mathbf{S}_n ,$$

where

$$\mathbf{A}_n = \int dV \left\{ \int d\Omega \left[\frac{1}{\sigma} (\hat{\Omega}\bullet\vec{\nabla}\mathbf{f})(\hat{\Omega}\bullet\vec{\nabla}\mathbf{f})^T + \sigma \mathbf{f}\mathbf{f}^T \right] - \sigma_s \mathbf{f}\mathbf{f}^T \right\} ,$$
$$\mathbf{M}_n = \int d\Gamma_n \int d\Omega\, \hat{n}\bullet\Omega\, \mathbf{f}\mathbf{h}^T , \quad (13)$$
$$\mathbf{s}_n = \int dV \left\{ \int d\Omega\, \mathbf{f}^T \mathbf{s} \right\} .$$

Requiring the forward functional F to be stationary with respect to ζ and χ yields the equations:

$$\begin{bmatrix} \mathbf{A} & \mathbf{M} \\ -\mathbf{M}^T & \mathbf{0} \end{bmatrix} \begin{bmatrix} \zeta \\ \chi \end{bmatrix} = \begin{bmatrix} \mathbf{s} \\ \mathbf{0} \end{bmatrix} \tag{14}$$

Similarly, requiring F* to be stationary with respect to ζ^* and χ^* yields the adjoint equations:

$$\begin{bmatrix} \mathbf{A} & -\mathbf{M} \\ \mathbf{M}^T & \mathbf{0} \end{bmatrix} \begin{bmatrix} \zeta^* \\ \chi^* \end{bmatrix} = \begin{bmatrix} \mathbf{s}^* \\ \mathbf{0} \end{bmatrix} \tag{15}$$

It is noteworthy that, because A is a symmetric matrix, the coefficient matrix of the adjoint equations is the transpose of the coefficient matrix of the forward equations. This is in contrast to other nodal methods where a transformation must be applied to convert the mathematical adjoint to the physical adjoint.

III. MULTIGROUP PERTURBATION EXPRESSIONS

To this point, we have treated only the within-group forward and adjoint equations. Before deriving the perturbation equations, we formulate (14) and (15) as global, multi-group equations. We expand the group sources, s and s*, into fission and group-to-group scattering matrices, $\tilde{\mathbf{F}}$ and $\tilde{\mathbf{C}}$, with the following group structure:

$$\tilde{\mathbf{F}} = \begin{bmatrix} \chi_1\nu_1\sigma_{f_1} & \chi_1\nu_2\sigma_{f_2} & \cdots & \chi_1\nu_g\sigma_{f_g} \\ \chi_2\nu_1\sigma_{f_1} & \cdots & & \\ \cdots & & & \\ \chi_g\nu_1\sigma_{f_1} & & & \chi_g\nu_g\sigma_{f_g} \end{bmatrix}, \quad \tilde{\mathbf{C}} = \begin{bmatrix} 0 & \sigma_{12} & \sigma_{13} & \cdots & \sigma_{1g} \\ \sigma_{21} & 0 & & & \\ \sigma_{31} & & \cdots & & \\ \cdots & & & & \\ \sigma_{g1} & & & & 0 \end{bmatrix},$$

where g is the energy group index. Next, we add a subscript g to the A and M matrices to indicate energy group and combine them into block diagonal supermatrices:

$$\tilde{\mathbf{A}} = \begin{bmatrix} \mathbf{A}_1 & \mathbf{0} & \mathbf{0} & \mathbf{0} \\ \mathbf{0} & \mathbf{A}_2 & \mathbf{0} & \mathbf{0} \\ \mathbf{0} & \mathbf{0} & \cdots & \mathbf{0} \\ \mathbf{0} & \mathbf{0} & \mathbf{0} & \mathbf{A}_g \end{bmatrix}, \quad \tilde{\mathbf{M}} = \begin{bmatrix} \mathbf{M}_1 & \mathbf{0} & \mathbf{0} & \mathbf{0} \\ \mathbf{0} & \mathbf{M}_2 & \mathbf{0} & \mathbf{0} \\ \mathbf{0} & \mathbf{0} & \cdots & \mathbf{0} \\ \mathbf{0} & \mathbf{0} & \mathbf{0} & \mathbf{M}_g \end{bmatrix}.$$

Similarly, we combine the forward and adjoint angular flux vectors for all energy groups.

$$\Psi^T = [\ \zeta_1\ \ \zeta_2 \cdots \zeta_g\ \chi_1\ \chi_2\ \cdots\ \chi_g\ ],$$
$$\Psi^{*T} = [\ \zeta_1^*\ \ \zeta_2^* \cdots \zeta_g^*\ \chi_1^*\ \chi_2^*\ \cdots\ \chi_g^*\ ].$$

We now combine equations (14) and (15) with these definitions to obtain a single multi-group equation

$$[\mathbf{A} + \mathbf{M}]\ [\Psi] = \left[\frac{1}{k}\mathbf{F} + \mathbf{C}\right][\Psi] \tag{16}$$

and the corresponding adjoint equation

$$[A + M^T]\,[\Psi^*] = \left[\frac{1}{k} F^T + C^T\right][\Psi^*], \tag{17}$$

where we have further compacted the notation by defining

$$A = \begin{bmatrix} \tilde{A} & 0 \\ 0 & 0 \end{bmatrix},\ M = \begin{bmatrix} 0 & \tilde{M} \\ -\tilde{M}^T & 0 \end{bmatrix},\ F = \begin{bmatrix} \tilde{F} & 0 \\ 0 & 0 \end{bmatrix},\ \text{and}\ C = \begin{bmatrix} \tilde{C} & 0 \\ 0 & 0 \end{bmatrix}.$$

Finally, we apply a perturbation and write the perturbed forward equation as

$$[A' + M']\Psi' = \left[\frac{1}{k'} F' + C'\right]\Psi' \ , \tag{18}$$

where $A' = A + \delta A$, $M' = M + \delta M$, $k' = k + \delta k$, and so on.

To obtain an expression for the change in the eigenvalue, we first premultiply the perturbed forward equation (18) by the transposed adjoint flux

$$\Psi^{*T}[A' + M']\Psi' = \Psi^{*T}\left[\frac{1}{k'} F' + C'\right]\Psi' \quad , \tag{19}$$

Next we transpose the adjoint equation (17) and postmultiply by the perturbed forward flux

$$\Psi^{*T}[A + M]\Psi' = \Psi^{*T}\left[\frac{1}{k} F + C\right]\Psi' \ . \tag{20}$$

Subtracting equation (20) from (19) and rearranging, yields an exact expression for the perturbation in the critical eigenvalue

$$\frac{\delta k}{k'k} = \frac{\Psi^{*T}\left[\frac{1}{k'}\delta F + \delta C\right]\ \Psi' - \Psi^{*T}[\delta A + \delta M]\ \Psi'}{\Psi^{*T}\, F\, \Psi'} \ , \tag{21}$$

Exact perturbation theory, while necessary for ascertaining accuracy of the code, is also useful for problems with extremely small perturbations. Exact perturbation theory is insensitive to errors in the flux due to approximations of the method and is therefore more accurate for computing changes in eigenvalues with extremely small differences than subtracting the two eigenvalues directly.[10]

For small perturbations, a first order approximation of the eigenvalue perturbation is obtained by setting $k' \cong k$, expanding Ψ' into $\Psi + \delta\Psi$ and eliminating all second order terms. The expression becomes

$$\frac{\delta k}{k^2} = \frac{\Psi^{*T}\left[\frac{1}{k}\delta F + \delta C\right]\ \Psi - \Psi^{*T}[\delta A + \delta M]\ \Psi}{\Psi^{*T}\, F\, \Psi} \ . \tag{22}$$

IV. IMPLEMENTATION

Equations (21) and (22) serve as a basis for a post-processor code for VARIANT[11], the Argonne National Laboratory module for performing variational nodal calculations. The code combines cross section and geometry files with the forward and adjoint flux files from VARIANT to evaluate first order and/or exact perturbation expressions.

To test the post-processor, exact and first order perturbation calculations have been performed using equations (21) and (22) respectively. Two perturbations were applied to the three-dimensional Takeda Benchmark Model 1,[12] a small LWR shown in Fig. 1. The 2-group cross sections and energy structure can be found in reference 12. For the first example, the base configuration is the standard rods-out problem and the core configuration is altered by increasing the thermal capture cross section as a percentage of the base core total thermal cross section. The base for the second example is the rods-in case, and the perturbed configuration consists of increasing the thermal capture cross section of the material in the control rod region.

These perturbations represent changes in the cross sections only. The **M** matrix, as shown in equation (13), does not contain any cross sections and therefore, $\delta\mathbf{M} = 0$. As a result, the partial current moments, χ, are not necessary for the calculation of δk. Thus, the perturbation expressions are simpler than conventional nodal perturbation methods which require both fluxes and partial currents. Simplifying equations (21) and (22), we see that the perturbations depend only on the even-parity fluxes.

$$\frac{\delta k}{k'k} = \frac{\zeta^{*T}\left[\frac{1}{k'}\delta\mathbf{F} + \delta\mathbf{C}\right]\ \zeta' - \zeta^{*T}\,\delta\mathbf{A}\ \zeta'}{\zeta^{*T}\,\mathbf{F}\,\zeta'},$$

$$\frac{\delta k}{k^2} = \frac{\zeta^{*T}\left[\frac{1}{k}\delta\mathbf{F} + \delta\mathbf{C}\right]\ \zeta - \zeta^{*T}\,\delta\mathbf{A}\ \zeta}{\zeta^{*T}\,\mathbf{F}\,\zeta}.$$

For the calculations, a quartic spatial approximation on the internal flux and a linear spatial approximation on the flux at the interfaces were used; P_1 angular approximations internally and on the interfaces represent the diffusion approximation, and P_3 angular approximations were used for the transport calculations. The results of the VARIANT calculations as well as the exact and first order perturbation calculations using both diffusion and transport approximations are given in Table 1 and in Figures 2 and 3.

As expected, the forward and adjoint eigenvalues are equivalent within convergence criteria (10^{-6}). For the first example, we see that first order perturbation theory is quite accurate, even to very large perturbations in the critical eigenvalue. It is interesting to note that the δk from exact perturbation theory in the diffusion approximation gives a very accurate value useful for transport. Often, two VARIANT diffusion runs and one exact theory perturbation calculation are much faster than a first order perturbation calculation in transport due to the larger numbers of moments in the transport case. For problems such as the first example, one could perform exact diffusion calculations to estimate changes in the transport eigenvalue. In the second example, we have also perturbed the thermal capture cross section. For this case, first order perturbation is accurate for larger changes in the thermal capture cross section; however, the perturbation in the eigenvalue is extremely small. Here, we see that first order transport calculations give more accurate results for the linear portion of Fig. 3 than the exact diffusion results.

Although we apply the same cross section increases in both problems, the result of perturbing the material in the control rod region is much smaller. As shown in Fig. 3, first order theory breaks down after a very small $\delta k/k$. In cases where the applied perturbations are localized, flux shapes may be greatly affected while the eigenvalue is not. The absence of flux shape correction, therefore, renders first order perturbation theory ineffectual for such cases.

V. DISCUSSION

To formulate the perturbation method in three dimensions, we have incorporated trial functions in x-y-z. By deriving these functions in dimensionless form, we are able to generate them using a symbolic manipulator, MATHEMATICA once for a given geometry and then store the results in a subroutine. Furthermore, the three-dimensional formulation requires integration over an additional dimension. Therefore, each term in the perturbation formula was adjusted to incorporate the additional integral. Although the three-dimensional form allows us to study a wider variety of more realistic problems, the increase in the number of nodes and the number of moments greatly increases the computation times. Possible methods for decreasing computation times are being explored. Future work on the perturbation method for the VNM will focus on extensions to hexagonal-z geometry and anisotropic scattering. Inclusion of the treatment of more types of perturbations as well as the extension to generalized perturbation theory are being considered.

ACKNOWLEDGEMENTS

The authors gratefully acknowledge C. Carrico and G. Palmiotti of Argonne National Laboratory for their assistance with VARIANT.

REFERENCES

1. C.B. Carrico, E.E. Lewis, and G. Palmiotti, "Three-Dimensional Variational Nodal Transport Methods for Cartesian, Triangular and Hexagonal Criticality Calculations," *Nucl Sci. Eng.*, **111**, 168 (1992).

2. K.L. Derstine, "DIF3D: A Code to Solve One-, Two-, and Three-Dimensional Finite Difference Diffusion Theory Problems," ANL-82-64, Argonne National Laboratory (Apr. 1984).

3. R.D. Lawrence, "Perturbation Theory within the Framework of a Higher Order Nodal Method," *Trans. Am. Nucl. Soc.*, **46**, 402 (1984).

4. T.A. Taiwo, A.F. Henry, "Perturbation Theory Based on a Nodal Method," *Nucl. Sci. Eng.*, **92**, 34 (1986).

5. T.A. Taiwo, "Mathematical Adjoint Solution to the Nodal Code QUANDRY,"*Trans. Am. Nucl. Soc.*, **55**, 580 (1987).

6. W.S. Yang, "Similarity Transformation Procedure for Nodal Adjoint Calculations," *Trans. Am. Nucl. Soc.*, **66**, 270 (1992).

7. W.S. Yang, T.A. Taiwo, and H. Khalil, "Solution of the Mathematical Adjoint Equations for an Interface Current Nodal Formulation," *Nucl. Sci. Eng.*, **116**, 42 (1994).

8. K. Laurin-Kovitz, E.E. Lewis, "The Adjoint Variational Nodal Method," *Trans. Am. Nucl. Soc.*, **69**, 210 (1993).

9. K. Laurin-Kovitz, E.E. Lewis, "Eigenvalue Perturbation Calculations for the Variational Nodal Method,"*Trans. Am. Nucl. Soc.*, **70**, 161 (1994).

10. M.L. Williams, "Perturbation Theory for Nuclear Reactor Analysis," CRC Handbook of Reactors Calculations, Y. Ronen, ed., Vol III., pp.63-188, CRC Press, (1986).

11. G. Palmiotti, C.B. Carrico, and E.E. Lewis, "Variational Nodal Transport Methods with Anisotropic Scattering," *Nucl. Sci. Eng.*, **115**, 233 (1993).

12. T. Takeda et al., "3-D Neutron Transport Benchmarks," NEACRP-L-330, OECD/NEA (1991).

TABLE 1: EIGENVALUES FOR TAKEDA BENCHMARK MODEL 1 PERTURBATIONS

VARIANT approximation	$\delta\sigma_\gamma/\delta\sigma_{tot}$	Core Perturbations eigenvalues		Control Rod Perturbations eigenvalues	
		base	perturbed	base	perturbed
P_1 diffusion	.025	.928681	.822638	.931866	.931282
	.050		.741739		.930817
	.075		.678004		.930441
	.100		.626492		.930133
P_3 transport	.025	.976396	.864825	.962243	.961730
	.050		.779788		.961316
	.075		.712841		.960979
	.100		.658765		.960699

FIGURE 1: TAKEDA BENCHMARK MODEL 1 CORE CONFIGURATION

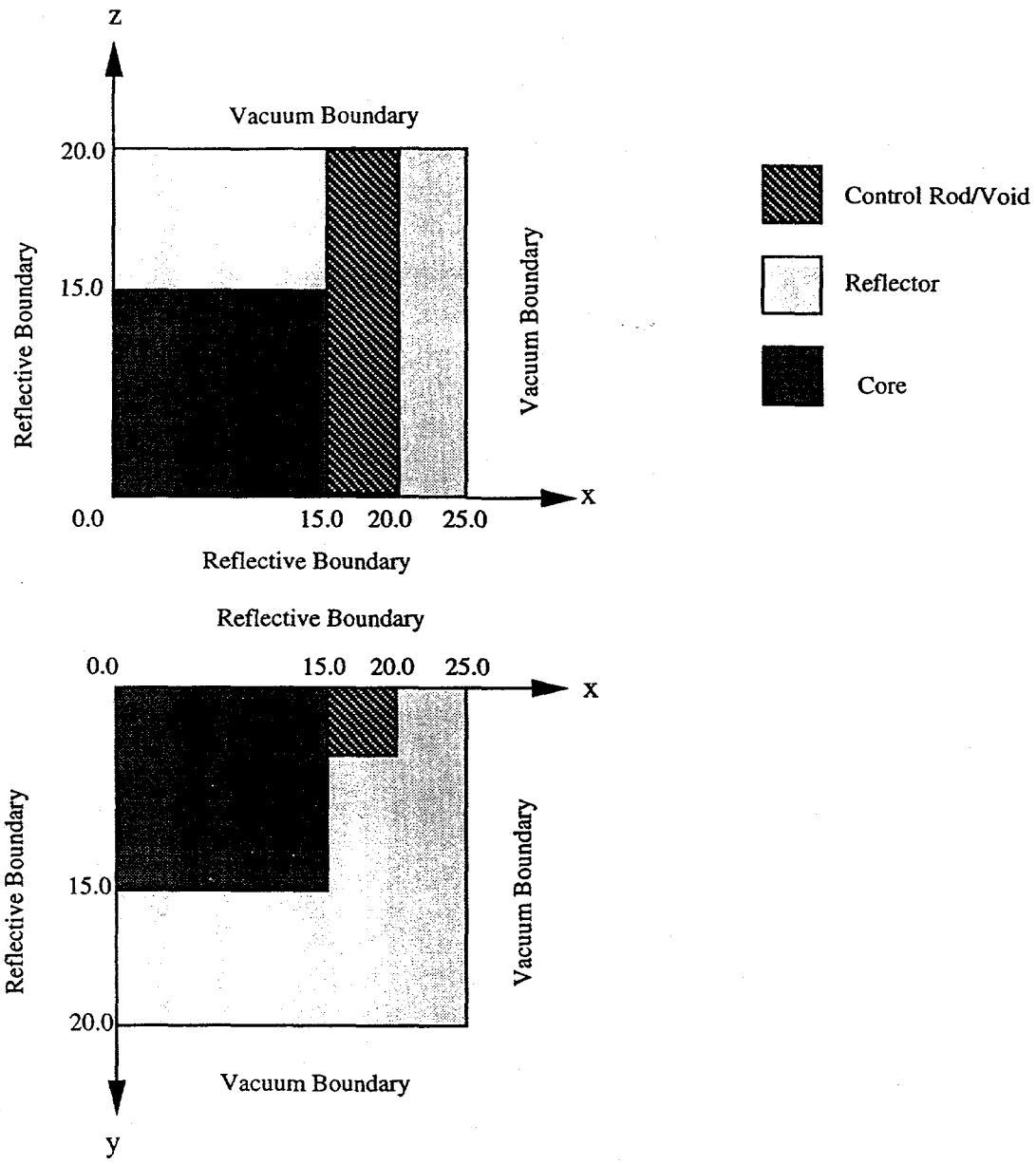

Figure 2: TAKEDA BENCHMARK 1
CORE PERTURBATION

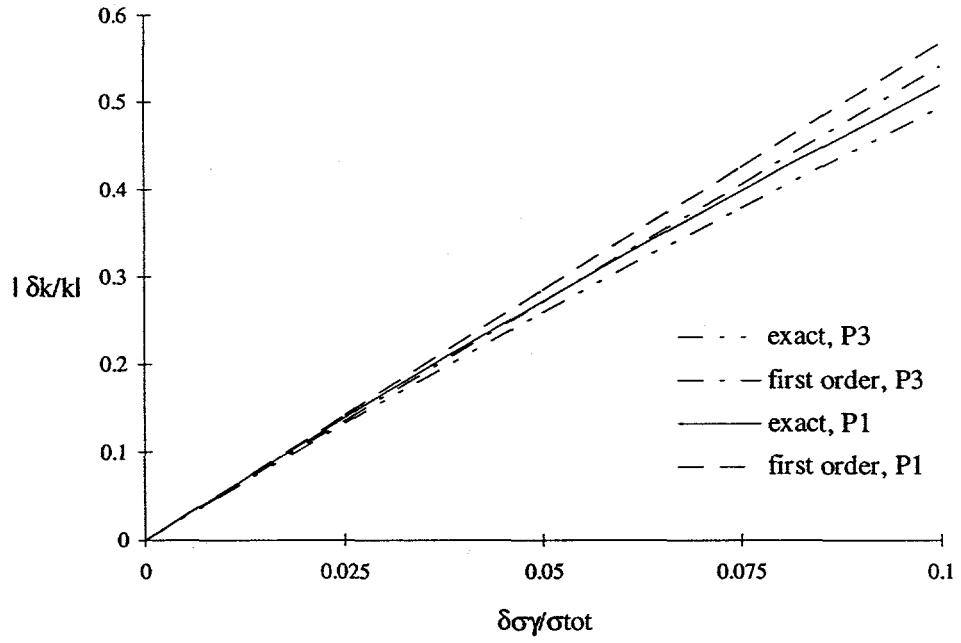

Figure 3: TAKEDA BENCHMARK 1
CONTROL ROD PERTURBATION